

Propagating RF phase: a new contrast to detect local changes in conductivity

A. L. van Lier¹, A. J. Raaijmakers¹, D. O. Brunner², D. W. Klomp³, K. P. Pruessmann², J. J. Lagendijk¹, and C. A. van den Berg¹

¹Radiotherapy, UMC Utrecht, Utrecht, Netherlands, ²Institute for Biomedical Engineering, ETH Zurich, Zurich, Switzerland, ³Radiology, UMC Utrecht, Utrecht, Netherlands

Introduction: The propagating RF phase ($\angle B_1^+ B_1^-$, [1]) is often encountered as a disadvantage in MRI, because it causes a spatially varying excitation pattern due to interference between the fields. In this abstract we use the propagating RF phase to our advantage, since it contains information about the local permittivity and especially conductivity. This new contrast can be used to image structures with higher (or lower) conductivity than its surrounds such as CSF and more clinically relevant high conducting breast tumours [2].

Theory: From basic EM theory we know that the wavelength, thus the propagating phase, depends on the permittivity and conductivity. For simple structures we can calculate the effect of local differences algebraically, but for complex structures as the head, we have to solve the problem numerically, for example using FDTD. Our first interest was to determine if contrast in the propagating RF phase is mainly due to changes in the local conductivity (σ) or the relative permittivity (ϵ_r). We investigated the effect at 7T by simulating a sphere ($r = 7.5$ cm, $\sigma = 1$ S/m $\epsilon_r = 40$) containing a smaller sphere ($r = 2$ cm) with different conductivities (0.005, 0.5, 1.0, 1.5 and 2.0 S/m) and relative permittivities (1, 20, 40, 60, 80) within the physiological range. The results of these simulations are shown in figure 1. To visualize the effect, we show a subtraction with a sphere without contrast (inner sphere: $\sigma = 1$ S/m $\epsilon_r = 40$), to remove the global RF phase. In this overview we see clearly that the conductivity has the largest contribution to the local RF phase in the investigated range. Therefore we focus on contrast in conductivity in the rest of this abstract.

Methods: The effect of the local changes in conductivity on the propagating RF phase were simulated using FDTD. The geometry of interest was placed in a 7T high-pass birdcage coil. Measurements were performed in a 7T scanner (Achieva, Philips Medical Systems, Best, the Netherlands) using the same head coil. We measured the propagating RF phase by extracting ϕ_0 contributions from the signal phase [3] using two separate GRE measurements with a different TE (TE1 = 2ms, TE2 = 3ms, TR = 300ms, resolution phantom 2x2x5mm, resolution *in vivo* 2.5x2.5x5 mm), while keeping all other parameters constant. To prevent phase wraps, B0 shimming was applied. To improve sensitivity we increased NSA (phantom: 32, *in vivo*: 2). The measurement time was in the order of minutes.

Materials: The effect was measured in a phantom consisting of two coaxial cylinders filled with agarose gel. The boundary between the cylinders consists of a 65 μ m thick layer of rubber-latex. Three of these phantoms were constructed; in the inner cylinder NaCl (0 g/L, 5g/L and 10g/L) was added to the gel to increase the conductivity ($\sigma = 0.04, 0.9$ and 1.73 S/m, resp.). To measure the effect *in vivo* we choose the head, which contains the ventricles, a cavity filled with the highly conducting CSF (cerebrospinal fluid, $\sigma = 2.22$ S/m). The ventricles are surrounded by the less conducting white matter (WM, 0.41 S/m).

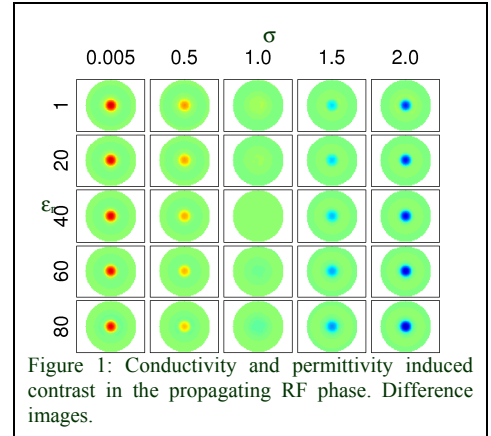


Figure 1: Conductivity and permittivity induced contrast in the propagating RF phase. Difference images.

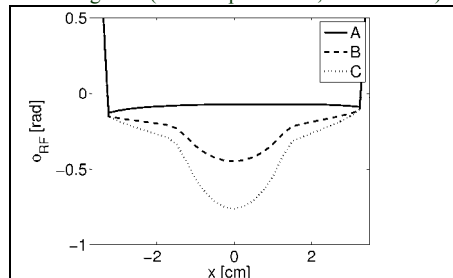


Figure 2: FDTD simulations of the RF phase for the coaxial phantom. A) $\sigma_{inner} = 0.04$ S/m B) $\sigma_{inner} = 0.9$ S/m C) $\sigma_{inner} = 1.73$ S/m

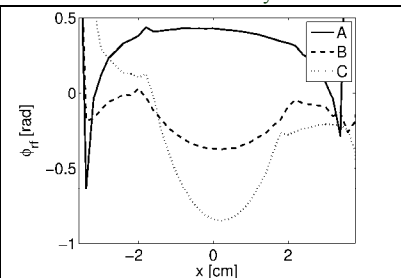


Figure 3: Measurement of the RF phase for the coaxial phantom. A) $\sigma_{inner} = 0.04$ S/m B) $\sigma_{inner} = 0.9$ S/m C) $\sigma_{inner} = 1.73$ S/m

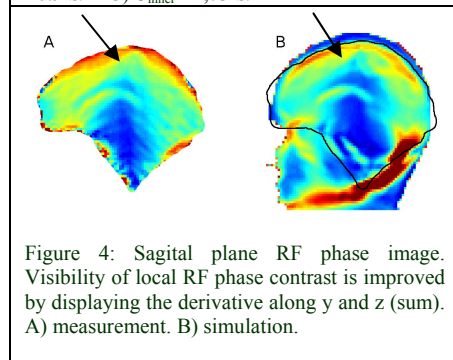


Figure 4: Sagittal plane RF phase image. Visibility of local RF phase contrast is improved by displaying the derivative along y and z (sum). A) measurement. B) simulation.

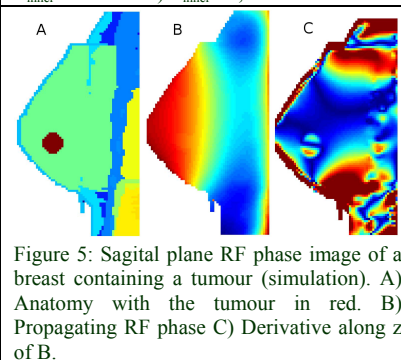


Figure 5: Sagittal plane RF phase image of a breast containing a tumour (simulation). A) Anatomy with the tumour in red. B) Propagating RF phase C) Derivative along z of B.

Results: In figure 2 and 3 we show the results of the phantom measurements. Here it is shown that the increase in RF phase contrast for a higher conductivity as predicted by the simulations (figure 2) is also measured (figure 3). In figure 4 we show the results of the *in vivo* measurements. For visibility purposes we show the derivative of the propagating phase for the head measurements, because the large global variation of the phase obscures the small local changes. At the location of the ventricle (indicated by the arrow) a local minimum in the derivative of the RF phase is present, in the simulations (B) as well as the measurements (A).

Conclusion and discussion: We have shown, that it is possible to measure local variations in the propagating RF phase, which is most strongly present in case of contrast in conductivity. We were able to measure the effect in phantoms and *in vivo* with good correlation with simulations. To visualize local changes in the RF phase, one needs to remove the global RF phase behaviour. Here we have shown images based on the derivative, which improves contrast. A possible application of this technique is shown in a simulation in figure 5. In these simulations a fatty breast containing a sphere-like tumour with a high conductivity (0.9 S/m) as found in breast cancer literature is simulated for a quadrature dual loop coil [2,4]. In the post-processed image (figure 5 C) the tumour location is clearly visible. Therefore this technique might be very useful in detecting conducting malignancies.

[1] Hoult, Concepts in Magnetic Resonance, 2000, 12 pp. 173-187
 [2] Lin, Advances in Electromagnetic Fields in Living Systems, Springer Science+Business Media, Inc. 2005 pp. 50-51
 [3] Haacke et al., Magnetic Resonance Imaging: Physical Principles and Sequence Design, John Wiley & Sons, Inc., 1999 pp. 758
 [4] Klomp et al. Proc. ISMRM, 2009, 2367